Reply to the Reviewer of Manuscript EGUSphere-2025-2600:

We would like to sincerely thank the editor and reviewer for their time, effort, and thoughtful feedback on our manuscript. The reviewer comments are shown in **blue**, with the authors' responses shown in **black** and any edited manuscript language shown in *italicized black font*.

General Comments

This study beautifully documents the deep convective clouds that occur almost daily during summer over the Magdalena Mountains, which serve as a natural laboratory for continental convection. I enjoyed reading the detailed descriptions, which provide a comprehensive account and interpretation of the observations surrounding and within these clouds. The study describes the differences and probable causes of the aerosols, thermodynamics, and composition of the clouds under different air mass origins. These clouds, unsurprisingly, have high and cold bases, microphysically highly continental, with little or no significant warm rain processes. It follows that the clouds remain supercooled at least up to the -20 °C isotherm, which was the top of the measured flight levels. Apparently, only growing cloud towers were penetrated, because maturing clouds do glaciate at least occasionally at these high supercooled temperatures as they mature. So, please clarify the selection criteria for cloud penetrations.

We thank the reviewer for highlighting this important point.

The aircraft penetrations were not random but specifically guided by flight planning and operational constraints. Actively growing convective towers were preferentially sampled using real-time data and communication from the cloud radar network operators. In situ aircraft video was employed to provide an aircraft discussion to identify potential developing towers for sampling. These provided the best opportunity to capture supercooled liquid water and the early-stage microphysical evolution and ice processes. In contrast, mature or dissipating clouds were generally avoided or departed from, because of their lower likelihood of containing significant supercooled water, and stronger turbulence hazards for safe aircraft operations. Outflow regions following convective development were also identified for sampling when possible. Therefore, our dataset primarily represents developing cloud stages, which explains why full glaciation was rarely observed. In summary, the sampling strategy focused on early to middevelopment stages of convective clouds, where cloud tops were supercooled to at least –20 °C. This sampling strategy explains why complete glaciation was generally not encountered within the penetrated clouds, even though such processes could occur in maturing convective elements in the region.

The authors have added the related description in the method section:

"The sampling strategy focused on early to mid-development stages of convective clouds with supercooled tops. Mature or dissipating clouds were generally avoided or departed from, because of their lower likelihood of containing significant supercooled water, and stronger turbulence hazards for safe aircraft operations. As a result, complete glaciation was rarely encountered within the penetrated clouds, even though it occurred in maturing convective elements in the region."

The most enlightening part of the paper was the comparison of the clouds' vertical microphysical profiles with the parcel model, considering various assumptions. It showed the potential role of mixing in cloud drop activation and evaporation aloft. While informative, the paper lacks a scientific focus and a statement of novelty, i.e., where does it contribute fundamental understanding to the state of the art? This is evident in the fact that much of the introduction is devoted to issues not addressed by the findings of this study, such as the extensive description of the aerosol convective invigoration hypothesis.

This shortcoming can be overcome by focusing on the processes of cloud mixing (homogeneous vs. inhomogeneous) and the additional activation of drops versus evaporation aloft. To do that, I suggest:

- 1. Replace much of the irrelevant parts of the introduction with a review of the known background on the processes that cause deviations from adiabatic parcels in deep non-precipitating water clouds.
- 2. Review causes for shaping the cloud drop size distributions with height in such clouds.

Thanks to the reviewer for raising these insightful points.

Regarding suggestions-1&2: We have re-organized the introduction:

- 1) The introduction of invigoration hypothesis has been deleted.
- 2) We now emphasize that detailed characterization of aerosol amounts and properties is crucial for understanding the droplet formation and development in deep convective systems. Moreover, atmospheric sources and transport generate temporally varying aerosol types, amounts, and properties in a given region.
- 3) We have added the background on how entrainment processes and aerosol mixing affect the development of convective clouds.

The revised introduction is:

"The life cycle of deep convective clouds is modulated by complex microphysical processes, including droplet formation, droplet growth through condensation and coalescence, thermodynamic phase transitions between liquid droplets and ice crystals, and the development of precipitation (Arakawa, 2004). Aerosols play a key role in these processes, and aerosol-cloud interactions are considered among the largest uncertainties in estimating climate sensitivity to radiative forcing (Boucher et al., 2013; Forster et al., 2021). Aerosols can affect clouds by acting as cloud condensation nuclei (CCN) or ice nucleating particles (INP), which is termed aerosol indirect effects (Boucher et al., 2013). In the presence of aerosols or sufficient CCN, water vapor condenses onto CCN surfaces to form cloud droplets, marking the initial process in the lifecycle of convective clouds that mostly occurs at cloud base (Tao et al., 2012; Rosenfeld et al., 2014). Generally, higher CCN concentrations produce a greater number of smaller droplets and narrower droplet size distributions, which are likely to inhibit collision-coalescence and delay raindrop formation, thereby extending cloud lifetime (Rosenfeld, 2000; Tao et al., 2012). This delay can have opposing effects on convective cloud development: the increased condensational heat release tends to enhance cloud buoyancy and vertical development, while the resulting increase in condensate loadings partially offsets that buoyancy enhancement (Rosenfeld et al., 2008; Koren et al., 2014; Fan et al., 2018; Varble et al., 2023). However, the presence of giant CCN, such as coarse-mode sea salt aerosols, can produce initially large droplets and accelerate warm rain formation, thereby inhibiting the vertical development of convective clouds (Yin et al., 2024). These existing studies suggest that the CCN ability of aerosols determines the initial droplet number concentration and size distributions, thereby influencing subsequent cloud dynamics throughout convective cloud lifetime. Additionally, INPs can promote the heterogeneous freezing, and regulate ice crystal number concentrations during convective development (Tao et al., 2012). Detailed characterization of aerosol amounts and properties is therefore crucial for improving the representation of aerosol-cloud interactions in atmospheric models, in particular, aerosol size distribution and chemical composition which determine their CCN and INP ability (Petters and Kreidenweis, 2007). However, the representation of aerosol properties and associated indirect effects is complex and uncertain, as they are subject to atmospheric dynamic and thermodynamic conditions (Yang et al., 2020). Atmospheric transport generates temporally varying aerosol types, amounts, and properties in a given region (Yang et al., 2020). Moreover, cloud response to aerosol perturbations depends on environmental conditions, such as cloud-base temperature, updraft velocity, and humidity (Pruppacher and Klett, 2010). Previous studies have indicated that clouds with cool, high bases tend to exhibit little sensitivity in cloud-top height and precipitation to aerosol loadings, while clouds with warm, low bases display larger aerosol-induced changes (e.g. Li et al., 2011). Overall, it is critical to understand how varying aerosol properties influence convective cloud microphysics under different environmental conditions.

Another key uncertainty in understanding the development of convective clouds is the entrainment and mixing process. Theoretically, cloud-droplet growth in a closed (adiabatic) parcel leads to narrower size distributions as vertical development progresses, tending to suppress the onset of coalescence through differential gravitational sedimentation (Pruppacher and Klett, 2010). However, observations have revealed that cloud-droplet size distributions are relatively broader than those in ideal adiabatic parcels, and this result is usually attributed to a consequence of entrainment and mixing and secondary activation (Blyth, 1993; Chandrakar et al., 2016). Despite its recognized importance, the representation of the entrainment and mixing process in models remains uncertain. It is suggested that inhomogeneous mixing typically dominates when cloud droplets are small, as their evaporation rates significantly exceed the mixing rate of clouds with surrounding subsaturated air (Pruppacher and Klett, 2010). In this way, a subset of cloud droplets evaporates completely, leaving the others in the volume unchanged. When cloud droplets are larger and their evaporation rates are comparable to the mixing rate, homogeneous mixing dominates the system and the influence of inhomogeneous mixing weakens (Pruppacher and Klett, 2010). With homogeneous mixing, droplets evaporate by uniformly reducing their size across the population, leaving droplet number density largely unchanged except through simple dilution. While some studies suggest that entrainment and mixing in convective clouds are almost completely inhomogeneous (e.g. Burnet and Brenguier, 2007; Braga et al., 2017a), some other studies propose that inhomogeneous mixing may dominate early cloud development when droplets are small, and then homogeneous mixing may become more prevalent as convective clouds evolve (e.g. Lehmann et al., 2009). It is unclear whether the entrainment is predominantly homogeneous mixing, inhomogeneous mixing, or a combination of both. An improved understanding of how these mixing mechanisms dominate throughout the development of convective clouds is essential for improving the representation of their microphysical processes. Moreover, the consequence of entrainment processes on cloud microphysical evolution can be regulated by surrounding environmental conditions, such as relative humidity (RH) and aerosol characteristics (Koren et al., 2010). In particular, aerosols entrained with surrounding air can act as additional CCN and promote secondary activation of droplets above cloud base. Such additional activation has been identified as an important factor contributing to the broadening of droplet size distributions, toward small droplet diameters (Lehmann et al., 2009; Chandrakar et al., 2016). An improved understanding of aerosol entrainment will reduce the current uncertainty in predicting droplet number concentrations and size distributions."

3. In the parcel simulations, provide the exact handling, formulation, and fraction of mixing with ambient air and secondary aerosol activation. Which extent of mixing would provide the best match with observations? Would replacing the aerosol size distribution near cloud base with its vertical profile improve the agreement between the simulated and observed cloud microstructure vertical profile?

Regarding suggestion-3, we have revised the manuscript in four aspects as below:

1) The authors have added the exact handling and formulation of mixing with ambient air and secondary aerosol activation in the supplementary. The added supplementary is:

"S1 Representation of entrainment

In this study, two types of entrainment processes are considered: homogeneous and inhomogeneous mixing. For homogeneous mixing, entrained subsaturated air uniformly mixes with and dilutes the cloud parcel, leading to a uniform reduction in droplet size. When humidity decreases sufficiently to induce droplet evaporation, the released aerosol particles may reactivate. These processes are implemented by including additional formulations in the solver routine that are passed to variable-coefficient ordinary differential equation (VODE) solver. The related formulations are described in Pruppacher and Klett (2010, chapter 12). In brief, we assume a "jet" parcel, which allows entrainment to occur through the front interface of the plume. For a jet parcel with mass (m), density (ρ), radius (R_i)

and vertical velocity (W), entrainment is described in terms of a change in mass flux $F_m = \pi R_j^2 \rho W$ along the vertical plume axis. The change in mass flux over a vertical distance Δz is expressed as $\Delta z (dF_m/dz)$, from which $dF_m = 2\pi R_i \rho W dR_i$. The entrainment rate for a jet (μ_i) is therefore

$$\mu_j = \frac{1}{F_m} \frac{\mathrm{d}F_m}{\mathrm{d}z} = \frac{C}{R_j} \tag{S1}$$

where C is the important entrainment parameter, which is set as 0.2 based on previous laboratory studies. Entrainment will cause the parcel volume to increase with time. The parcel acceleration is calculated by considering the buoyancy and reaction of the surrounding air:

$$\frac{\mathrm{d}W}{\mathrm{d}t} = \frac{\mathrm{g}}{1+\gamma} \left(\frac{T-T'}{T'} - w_L \right) - \frac{\mu_j}{1+\gamma} W^2 \tag{S2}$$

where $\gamma \approx 0.5$, g is the acceleration due to gravity ($g \approx 9.80665$ m s⁻²), w_L is the liquid water mixing ratio, T is the temperature of air parcel, and T' is the ambient temperature of the surrounding air. For a jet parcel, we can also relate the growth of the radius to the entrainment rate μ_i according to

$$\frac{\mathrm{dln}R_j}{\mathrm{d}t} = \frac{1}{2} \left[\mu_j W - \frac{\mathrm{dln}\rho}{\mathrm{d}t} - \frac{\mathrm{dln}W}{\mathrm{d}t} \right] \tag{S3}$$

which represents parcel dilution, expansion, and the conservation of mass flux, with $\frac{d\rho}{dt}$ expressed in terms of pressure and temperature derivatives using the ideal gas law. The condensed water is related to the water vapour mixing ratio (w_v) , through an obvious statement of water conservation, this leads to

$$\frac{dw_v}{dt} = -\frac{dw_L}{dt} - \mu_j(w_v - w_v' + w_L)W \tag{S4}$$

Where w_L is the liquid water mixing ratio and w_v' is the ambient water vapour mixing ratio of the surrounding air. For the settings of aerosols, we initially set a number size distribution of dry aerosol particles $(n_{AP,a}^{'})$ with mass $(m_{AP}^{'})$, where $n_{AP,a}(m_{AP})$ is the number distribution of inactivated drops inside the air parcel at a time t. The $n_{AP,a}(m_{AP})$ changes are due to (1) entrainment of additional aerosol particles from the environmental air, (2) the activation of some of the aerosol particles to drops, and (3) drops which by evaporation become deactivated particles again. These changes are considered in simulations, which are expressed by

$$\frac{\partial n_{AP,a}(m_{AP})}{\partial t} = -\mu_{j}W[n_{AP,a}(m_{AP}) - n'_{AP,a}(m_{AP})] + \frac{\partial n_{AP,a}(m_{AP})}{\partial t}\bigg|_{\text{activated/deactivated}}$$
(S5)

For inhomogeneous mixing, entrained subsaturated air remains in localized pockets rather than mixing instantaneously, leading to the evaporation of some droplets while others out of the pockets are unaffected. These processes are carried out outside the VODE solver, over a longer 10s timestep. The related formulations are the same as in the homogeneous mixing case (Eqs. S1-S5). For inhomogeneous mixing, the droplet number concentrations in each size bin are adjusted to conserve the parcel humidity, preventing a uniform reduction in droplet size as in the homogeneous mixing. When inhomogeneous mixing causes droplet evaporation, aerosol particles are released back into the discrete packets of subsaturated air, within the parcel, which may become re-activated later."

2) The mixing with ambient air is indicated by the strength of simulated entrainment rate (μ_j) . The vertical profiles of simulated μ_i are now shown in Fig. S8.

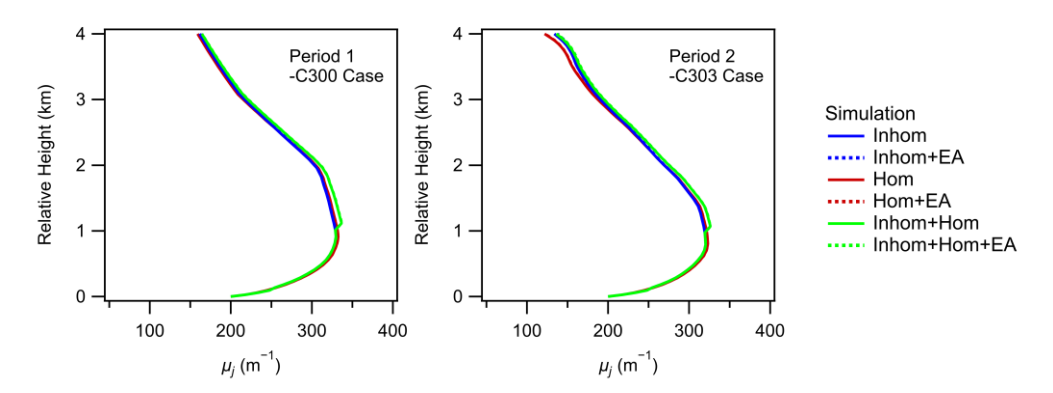


Figure S8. Vertical profiles of simulated μ_j (m⁻¹) for the Period 1-C300 case (left) and the Period 2-C303 case (right). The y-axis is the relative height with respect to the LCL height.

3) As described in the original manuscript, it is unclear whether mixing is predominantly homogeneous, inhomogeneous, or a combination of both. While some studies suggest that entrainment and mixing in convective clouds are almost completely inhomogeneous (e.g. Burnet and Brenguier, 2007; Braga et al., 2017a), some other studies propose that inhomogeneous mixing may dominate early cloud development when droplets are small, and then homogeneous mixing may become more prevalent as convective clouds evolve (e.g. Lehmann et al., 2009). In the revised manuscript, we examined three entrainment scenarios, including purely homogeneous mixing, purely inhomogeneous mixing, and a hybrid approach of early-stage inhomogeneous mixing (from the cloud base up to ~ 1 km above) followed by homogeneous mixing. We also examined the effects of aerosol entrainment. By comparing different scenarios, a combination of early-stage inhomogeneous mixing and following homogeneous mixing as well as the inclusion of aerosol entrainment would provide the best match with observations. The revised manuscript is:

"Many observations and modeling studies have suggested that entrainment and mixing processes are important for the evolution of cloud microphysics (Burnet and Brenguier 2007; Lehmann et al., 2009; Braga et al., 2017a). In this study, three entrainment scenarios were examined, including purely homogeneous mixing (denoted as "Hom"), purely inhomogeneous mixing ("Inhom"), and a hybrid approach of early-stage inhomogeneous mixing (from the cloud base up to ~ 1 km above) followed by homogeneous mixing ("Inhom+Hom"). In the simulations, the entrainment rate of surrounding air was constrained by thermodynamic profiles derived from dropsonde measurements. The simulated entrainment rates under different entrainment scenarios are shown in Fig. S8. With the inclusion of entrainment processes, which considered the dilution of cloud layers by entrained subsaturated air and the associated evaporation of cloud droplets, the simulated N_d and LWC were substantially reduced throughout the cloud depth compared to adiabatic simulations. As seen in Figs. 7a and 7b, the inclusion of entrainment improved the agreement between simulated and observed LWC profiles (red, blue, and green solid lines). Simulated cloud-base N_d values were more consistent with observations under the "Inhom" and "Inhom+Hom" scenarios (blue and green solid lines in Figs. 7c and 7d), whereas they were overestimated under the "Hom" scenario (red solid lines in Figs. 7c and 7d). However, all three scenarios exhibited a pronounced decrease in N_d with vertical development, in contrast to the relatively constant N_d in observations. Simulated R_e values were substantially overestimated under the "Inhom" and "Inhom+Hom" scenarios (blue and green solid lines in Figs. 7e and 7f), due to the underestimated N_d , particularly at higher cloud levels. The "Hom" scenario produced R_e profiles closer to observations (red solid lines in Figs. 7e and 7f) but continued to predict excessively narrow droplet size distributions (red solid lines in Fig. 8). All three entrainment scenarios failed to reproduce small cloud droplets as vertical development progressed (red, blue, and green solid lines in Fig. 8).

Previous studies suggest that aerosols entrained with surrounding subsaturated air can be activated in the rising air parcel, broadening droplet size distributions toward small droplet diameters (Lehmann et al., 2009; Chandrakar et al., 2016). To account for this effect, aerosol entrainment (EA) was further incorporated into the simulations under three entrainment scenarios, denoted as "Hom+EA," "Inhom+EA," and "Inhom+Hom+EA" (red, blue, and green dashed lines respectively in Figs. 7 and 8). The entrained aerosols were assumed to follow the same size distributions as those measured near the cloud base (Fig. S7). For both cases, the further inclusion of aerosol entrainment made a negligible difference to the simulated LWC under three entrainment scenarios. In the Period 1 case (C300), incorporating aerosol entrainment improved the consistency of simulated N_d profiles with observations, capturing the slight decrease at low cloud layers followed by relatively constant values aloft. In particular, the "Inhom+EA" and "Inhom+Hom+EA" scenarios produced N_d values close to observations, whereas the "Hom+EA" scenario still overestimated N_d. Aerosol entrainment also broadened the droplet size distributions under three entrainment scenarios, effectively filling the deficit in small-droplet populations. Under the "Hom+EA" scenario, the overestimated N_d resulted in fewer large cloud droplets and slightly underestimated R_{e_i} particularly at higher cloud levels. In contrast, the "Inhom+EA" scenario produced a higher concentration of large droplets relative to observations, as vertical development progressed. This is likely due to excessive collisioncoalescence in the simulations, as inhomogeneous mixing promotes the evaporation of some droplets while leaving others unaffected, thereby enhancing droplet growth and shifting the droplet size distribution toward larger diameters (Pruppacher and Klett, 2010). These results suggest that homogeneous mixing should be incorporated as vertical development progresses. Overall, the "Inhom+Hom+EA" scenario provided the best agreement with observed N_d and cloud droplet size. In the Period 2 case (C303), aerosol entrainment presented the same effects on simulated LWC, N_d , and cloud droplet sizes as in the Period 1 case. However, the two cases exhibited slightly different sensitivities to aerosol entrainment under the "Inhom+Hom+EA" scenario. While the simulated N_d , R_e and droplet size distributions showed good agreement with observations in the Period 1 case, the Re and largesize droplets were slightly underestimated in the Period 2 case due to the overestimated N_d as vertical development progressed."

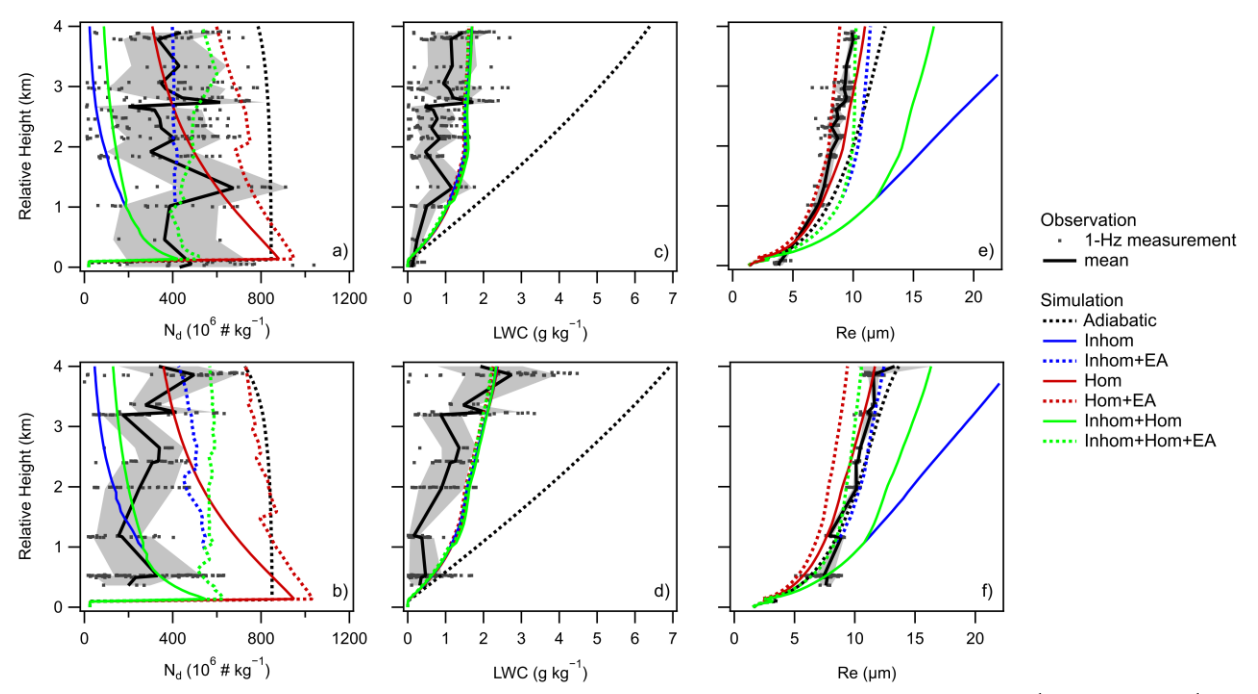


Figure 7. Vertical profiles of observed and simulated cloud droplet number concentration (N_d, kg^{-1}) , LWC $(g kg^{-1})$ and effective radius $(R_e, \mu m)$ for the Period 1-C300 case (upper plots) and the Period 2-C303 case (bottom plots). It is noted that,

for consistency with the model, the units of N_d and LWC are expressed in " kg^{-1} ", as opposed to " m^{-3} " in Sect. 3.3.1. The dots represent 1-hz measurements from the CDP. The solid black lines and shades represent averages and standard deviations of observed values. The dashed black, pink and green lines represent simulations under different scenarios respectively. The y-axis is the relative height with respect to the LCL height. It is noted that the pink and green dashed lines overlap in the plots of LWC.

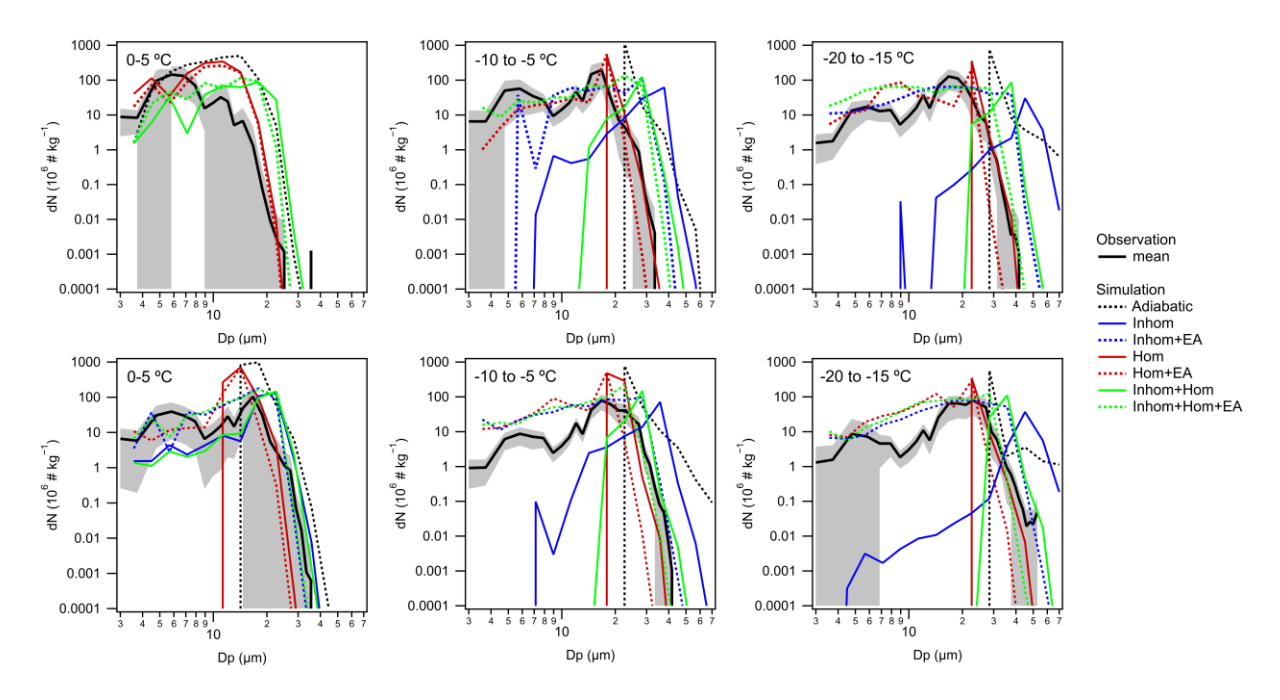


Figure 8. Observed and simulated cloud droplet size distributions for the Period 1-C300 case (upper plots) and the Period 2-C303 case (bottom plots), as a function of T ranging from near cloud base to high level. The solid black lines and shades represent averages and standard deviations of observed values within specific T ranges. The dashed black, pink, and green lines represent simulations under different scenarios, respectively.

4) Whether replacing the aerosol size distribution near cloud base with its vertical profile would improve simulations depends on the vertical variability of aerosol concentrations and size distributions. In the original manuscript, the entrained aerosols were assumed to follow the same size distributions as those measured near the cloud base. The further inclusion of aerosol entrainment made a negligible difference to the simulated LWC, however, the two cases in this study showed different responses in simulated N_d and cloud droplet size under the "Inhom+Hom+EA" scenario. In the Period 1 case (C300), Na and aerosol size distributions remained relatively constant above the cloud base. Consequently, the predicted N_d, R_e and widths of droplet size distributions showed good agreement with observations after accounting for aerosol mixing. In the Period 2 case (C303), Na decreased monotonically with height, and larger particles were less abundant above cloud base compared to measurements near cloud base. While the inclusion of aerosol entrainment improved simulations, the R_e and droplet size widths were slightly underestimated as vertical development progressed, due to an overestimation of N_d caused by excessive aerosol entrainment. Therefore, replacing the constant aerosol size distribution with its vertical profile would likely have little impact under Period 1 conditions but could improve the representation of droplet number and size evolution under Period 2 conditions. However, the SMPS measurements were recorded based on a ∼1 min averaging time. Given the low time resolution, SMPS analysis was only available during straight-and-level runs with relatively stable aerosol levels. As a result, our measurements didn't provide continuous vertical profiles of aerosol size distributions, but rather discrete measurements at specific altitudes. An alternative approach would be to incorporate fractional entrainment constrained by observed vertical profiles of aerosol number concentrations, which we plan to test in following studies. The revised manuscript is:

"However, the two cases exhibited slightly different sensitivities to aerosol entrainment under the "Inhom+Hom+EA" scenario. While the simulated N_d , R_e and droplet size distributions showed good agreement with observations in the Period 1 case, the R_e and large-size droplets were slightly underestimated in the Period 2 case due to the overestimated N_d as vertical development progressed. This discrepancy is likely due to different vertical profiles of aerosol concentrations and size distributions between the two cases. In the Period 1 case, N_a and aerosol size distributions remained relatively constant from the cloud base to above (Figs. S9a and b). In the Period 2 case, N_a decreased monotonically with height, and larger particles were less abundant above cloud base compared with measurements near cloud base (Figs. S9c and d). The assumption of constant aerosol size distributions during the entrainment process aligned well with the Period 1 case. However, it likely resulted in overestimated N_d in the Period 2 case, due to excessive entrained aerosols in simulations, which in turn led to underestimated R_e . Employing vertically resolved aerosol size distributions in the model would likely have little impact under Period 1 conditions but could improve the representation of droplet number and size evolution under Period 2 conditions.

Although our SMPS measurements did not provide continuous vertical profiles of aerosol size distributions due to limited time resolution, future studies should consider an approach of parameterizing fractional entrainment constrained by observed vertical profiles of aerosol number concentrations, to further improve model performance."

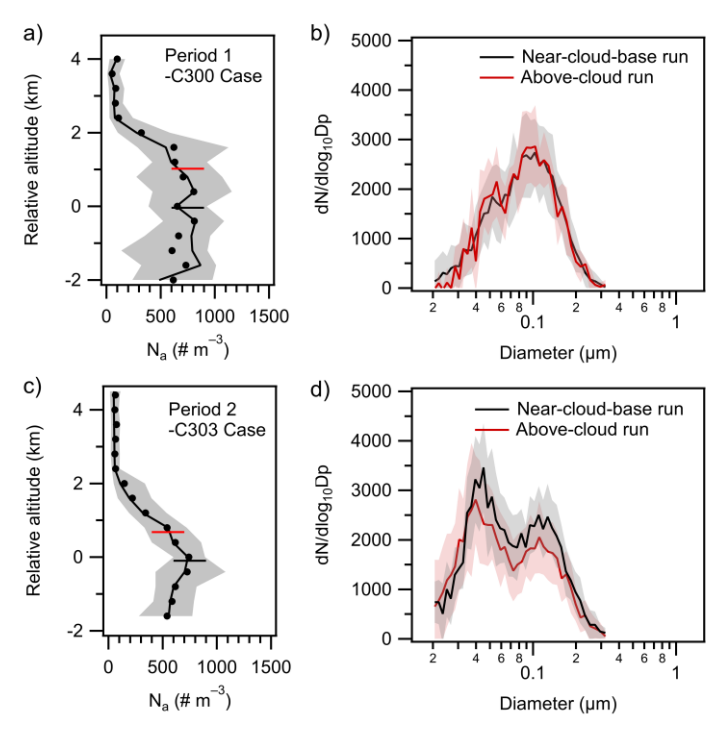


Figure S9. Vertical profiles of out-of-cloud N_a for a) the Period 1 case (C300) and c) the Period 1 case (C303). The lines, dots and shades represent median, mean, 10, and 90 percentiles. The black and red horizontal lines represent straight-and-level runs near the cloud base and above the cloud, respectively. The y-axis is the relative height with respect to the LCL height. b, d) Average aerosol size distributions during straight-and-level runs near the cloud base (black) and above the cloud (red) for b) the Period 1 case (C300) and d) the Period 1 case (C303). Lines and shades represent means and standard deviations.

4. Provide the formulation of the mix between homogeneous and inhomogeneous mixing, and which fractionation provides the best match to observations.

Regarding suggestion-4: The formulations for homogeneous and inhomogeneous mixing have been described in our response to suggestion-3, which are now included in the supplementary. In the revised manuscript, we examined three entrainment scenarios, including purely homogeneous mixing (denoted as "Hom"), purely inhomogeneous mixing ("Inhom"), and a hybrid approach of early-stage inhomogeneous mixing (from the cloud base up to ~ 1 km above) followed by homogeneous mixing ("Inhom+Hom"). Under the "Inhom+Hom" scenario, we did not implement homogeneous and inhomogeneous mixing simultaneously. The two types of mixing were treated sequentially, rather than as a combined process with prescribed fractional contributions. By comparing different scenarios, a combination of early-stage inhomogeneous mixing and following homogeneous mixing as well as the inclusion of aerosol entrainment would provide the best match with observations.

There is a wealth of data from the individual flights, warranting an additional study that focuses on this, aiming to find the parameterization that best fits the individual flights. It is likely beyond the scope of this paper, but at the very least, state that this is a potential future study when addressing the most general questions above.

Thanks to the reviewer for raising this insightful point. We agree that the extensive dataset obtained from individual flights offers valuable potential for developing general parameterizations that achieve improved agreement between simulations and observations. While this study focuses on case studies using a bin-microphysics parcel model to highlight the importance of incorporating aerosol entrainment, we are preparing a follow-up manuscript to conduct simulations for all flights during the DCMEX campaign. We will systematically investigate how different entrainment conditions (adiabatic, homogeneous, and inhomogeneous) affect not only cloud droplets but also secondary ice production.

We have expanded the discussion of implications; the revised conclusion is:

"Future simulation studies should be conducted for all flight cases, to develop general parameterizations that achieve improved agreement between models and observations. In addition, Future studies should investigate how different entrainment conditions (adiabatic, homogeneous, and inhomogeneous) affect not only the development of cloud droplets but also ice production."

Minor Comments

Line 395: It is much more likely that the SO₂ sources at the southeast are from urban and industrial emissions, including the extensive oil fields and refineries.

We thank the reviewer for this insightful comment. We have added the possible influence of urban and industrial SO₂ emissions in the southeast U.S. The rephrased manuscript is:

In addition, previous studies reported a relatively higher emission density of anthropogenic SO₂ and subsequent nearsurface sulfate concentrations in the eastern U.S. compared to the western U.S., largely due to emissions from power plants and industrial activities (Yang et al., 2017; Zhong et al., 2020). Therefore, both the marine emissions from the Gulf of Mexico and the large anthropogenic sulfur emission in the eastern U.S. likely contributed to the increase in sulfate levels in Period 2 under SE flow-controlled condition.

Line 500: Replace "raindrops" with "cloud drops". Accepted

Line 522: All cloud drop size distributions had a local maximum concentration at $6.5 \mu m$ and a local minimum at $8 \mu m$. It appears to be a problem of incorrect bin widths for the CDP, rather than a bimodal drop size distribution being the issue.

We thank the reviewer for this suggestion.

In the revised manuscript, we have done CDP calibrations following methods in previous FAAM studies (e.g. Barrett et al., 2022). The updated droplet size distributions (dN vs. Dp) continue to exhibit a generally bimodal structure (Fig. 8). We also plotted the CDP size distributions as dN/dlogDp vs. Dp (Fig. R1), which were normalized by bin width. Figure R1 also indicates a generally bimodal structure when bin-width normalization is applied.

However, to mitigate the concern proposed by the reviewer, we have rephrased the relevant sentence in the manuscript as follows:

"Observations of droplet size distributions typically presented wide ranges, with the width of size distributions increasing with height."

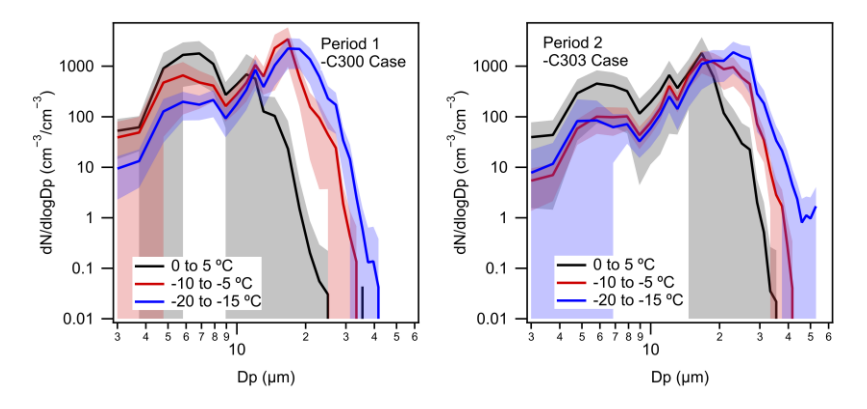


Figure R1. Observed cloud droplet size distributions for the Period 1-C300 case (left) and the Period 2-C303 case (right), as a function of T ranging from near cloud base to high level. The solid lines and shades represent the averages and standard deviations of observed values within specific T ranges.

Line 555 and the whole paragraph: How was the mixing performed in the model? And how was the portion of homogeneous and inhomogeneous mixing determined?

In the revised manuscript, we examined three entrainment scenarios, including purely homogeneous mixing (denoted as "Hom"), purely inhomogeneous mixing ("Inhom"), and a hybrid approach of early-stage inhomogeneous mixing followed by homogeneous mixing ("Inhom+Hom"). Under the "Inhom+Hom" scenario, we initiated the entrainment with inhomogeneous mixing from the cloud base up to approximately 1 km above it. Beyond this altitude, the simulations transitioned to homogeneous mixing. We did not implement homogeneous and inhomogeneous mixing simultaneously. The two types of mixing were treated sequentially under the "Inhom+Hom" scenario, rather than as a combined process with prescribed fractional contributions.

Lines 613-614: The added precipitation with warmer bases can be explained by the increased water vapor content and the corresponding additional condensation. Please add this as a further possible explanation.

We thank the reviewer for this suggestion. We have added the suggested explanation in the revised manuscript.

"The increased precipitation during the SE-flow period could also be attributed to elevated water vapor content at warmer and lower cloud bases, which promotes additional condensation."

Fig. S1: Please state the heights of the origins of the back tracks.

The release heights of the backward-dispersion simulations have been added to Fig. S1.

References

Arakawa, A.: The cumulus parameterization problem: Past, present, and future, J. Climate, 17, 2493–2525, https://doi.org/10.1175/1520-0442(2004)017<2493:RATCPP>2.0.CO;2, 2004.

Barrett, P. A., Abel, S. J., Coe, H., Crawford, I., Dobracki, A., Haywood, J., Howell, S., Jones, A., Langridge, J., McFarquhar, G. M., Nott, G. J., Price, H., Redemann, J., Shinozuka, Y., Szpek, K., Taylor, J. W., Wood, R., Wu, H., Zuidema, P., Bauguitte, S., Bennett, R., Bower, K., Chen, H., Cochrane, S., Cotterell, M., Davies, N., Delene, D., Flynn, C., Freedman, A., Freitag, S., Gupta, S., Noone, D., Onasch, T. B., Podolske, J., Poellot, M. R., Schmidt, S., Springston, S., Sedlacek III, A. J., Trembath, J., Vance, A., Zawadowicz, M. A., and Zhang, J.: Intercomparison of airborne and surface-based measurements during the CLARIFY, ORACLES and LASIC field experiments, Atmos. Meas. Tech., 15, 6329–6371, https://doi.org/10.5194/amt-15-6329-2022, 2022.

Blyth, A. M.: Entrainment in Cumulus Clouds, J. Appl. Meteorol., 32, 626–641, https://doi.org/10.1175/15200450(1993)032<0626:EICC>2.0.CO;2, 1993.

Boucher, O., Randall, D., Artaxo, P., Bretherton, C., Feingold, G., Forster, P., Kerminen, V.-M., Kondo, Y., Liao, H., Lohmann, U., Rasch, P., Satheesh, S.K., Sherwood, S., Stevens, B., and Zhang, X.-Y.: Clouds and aerosols, in: Climate change 2013: the physical science basis, Contribution of Working Group I to the Fifth Assessment Report of the Intergovernmental Panel on Climate Change, Cambridge University Press, 571–657, https://doi.org/10.1017/CBO9781107415324.016, 2013.

Braga, R. C., Rosenfeld, D., Weigel, R., Jurkat, T., Andreae, M. O., Wendisch, M., Pöhlker, M. L., Klimach, T., Pöschl, U., Pöhlker, C., Voigt, C., Mahnke, C., Borrmann, S., Albrecht, R. I., Molleker, S., Vila, D. A., Machado, L. A. T., and Artaxo, P.: Comparing parameterized versus measured microphysical properties of tropical convective cloud bases during the ACRIDICON–CHUVA campaign, Atmos. Chem. Phys., 17, 7365–7386, https://doi.org/10.5194/acp-17-7365-2017, 2017a.

Burnet, F. and Brenguier, J.-L.: Observational Study of the Entrainment-Mixing Process in Warm Convective Clouds, J. Atmos. Sci., 64, 1995–2011, https://doi.org/10.1175/JAS3928.1, 2007.

Chandrakar, K. K., Cantrell, W., Chang, K., Ciochetto, D., Niedermeier, D., Ovchinnikov, M., Shaw, R. A., and Yang, F.: Aerosol Indirect Effect from Turbulence-Induced Broadening of Cloud Droplet Size Distributions, P. Natl. Acad. Sci. USA, 113, 14243–14248, https://doi.org/10.1073/pnas.1612686113, 2016.

Forster, P., Storelvmo, T., Armour, K., Collins, W., Dufresne, J.L., Frame, D., Lunt, D., Mauritsen, T., Palmer, M., Watanabe, M., Wild, M., and Zhang, H.: The Earth's Energy Budget, Climate Feedbacks, and Climate Sensitivity, Cambridge University Press, Cambridge, United Kingdom and New York, NY, USA, https://doi.org/10.1017/9781009157896.009, 2021.

Koren, I., Feingold, G., and Remer, L. A.: The invigoration of deep convective clouds over the Atlantic: aerosol effect, meteorology or retrieval artifact?, Atmos. Chem. Phys., 10, 8855–8872, https://doi.org/10.5194/acp-10-8855-2010, 2010.

Koren, I., Dagan, G., and Altaratz, O.: From aerosol-limited to invigoration of warm convective clouds, Science, 344, 1143–1146, https://doi.org/10.1126/science.1252595, 2014.

Li, Z., Niu, F., Fan, J., Liu, Y., Rosenfeld, D., and Ding, Y.: Long-term impacts of aerosols on the vertical development of clouds and precipitation, Nat. Geosci., 4, 888–894, https://doi.org/10.1038/ngeo1313, 2011.

Petters, M. D. and Kreidenweis, S. M.: A single parameter representation of hygroscopic growth and cloud condensation nucleus activity, Atmos. Chem. Phys., 7, 1961–1971, https://doi.org/10.5194/acp-7-1961-2007, 2007.

Pruppacher, H. R. and Klett, J. D.: Microphysics of Clouds and Precipitation, in: 2nd Edn., Springer, Dordrecht, https://doi.org/10.1007/978-0-306-48100-0, 2010.

Rosenfeld, D.: Suppression of rain and snow by urban and industrial air pollution, Science, 287, 1793–1796, https://doi.org/10.1126/science.287.5459.1793, 2000.

Rosenfeld, D., Lohmann, U., Raga, G. B., O'Dowd, C. D., Kulmala, M., Fuzzi, S., Reissell, A., and Andreae, M. O.: Flood or drought: How do aerosols affect precipitation?, Science, 321, 1309–1313, https://doi.org/10.1126/science.1160606, 2008.

Rosenfeld, D., Sherwood, S., Wood, R., and Donner, L.: Atmospheric science. Climate effects of aerosol-cloud interactions, Science, 343, 379–380, https://doi.org/10.1126/science.1247490, 2014.

Tao, W., Chen, J., Li, Z., Wang, C., and Zhang, C.: Impact of aerosols on convective clouds and precipitation, Rev. Geophys., 50, RG2001, https://doi.org/10.1029/2011RG000369, 2012.

Varble, A. C., Igel, A. L., Morrison, H., Grabowski, W. W., and Lebo, Z. J.: Opinion: A critical evaluation of the evidence for aerosol invigoration of deep convection, Atmos. Chem. Phys., 23, 13791–13808, https://doi.org/10.5194/acp-23-13791-2023, 2023.

Yang, Y., Wang, H., Smith, S. J., Easter, R., Ma, P.-L., Qian, Y., Yu, H., Li, C., and Rasch, P. J.: Global source attribution of sulfate concentration and direct and indirect radiative forcing, Atmos. Chem. Phys., 17, 8903–8922, https://doi.org/10.5194/acp-17-8903-2017, 2017.

Yang, Y., Lou, S., Wang, H., Wang, P., and Liao, H.: Trends and source apportionment of aerosols in Europe during 1980–2018, Atmos. Chem. Phys., 20, 2579–2590, https://doi.org/10.5194/acp-20-2579-2020, 2020.

Yin, J., Pan, Z., Mao, F., Rosenfeld, D., Zhang, L., Chen, J., and Gong, J.: Large effects of fine and coarse aerosols on tropical deep convective systems throughout their lifecycle, npj Clim Atmos Sci, 7, 195, https://doi.org/10.1038/s41612-024-00739-6, 2024.

Zhong, Q., Shen, H., Yun, X., Chen, Y., Ren, Y., Xu, H., Shen, G., Du, W., Meng, J., Li, W., Ma, J., and Tao, S.: Global Sulfur Dioxide Emissions and the Driving Forces, Environ. Sci. Technol., 54, 6508–6517, https://doi.org/10.1021/acs.est.9b07696, 2020.